Fish & Shellfish Immunology 67 (2017) 561–570

Contents lists available at ScienceDirect

Fish & Shellfish Immunology

journal homepage: www.elsevier.com/locate/fsi

Full length article

A truncated Sph_{12-38} with potent antimicrobial activity showing resistance against bacterial challenge in *Oryzias melastigma*

Xiao-Wan Ma [a], Lin Hou [a], Bei Chen [a], Dan-Qing Fan [a], Yan-Chao Chen [a], Ying Yang [a], Ke-Jian Wang [a, b, c, *]

[a] State Key Laboratory of Marine Environmental Science, College of Ocean & Earth Science, Xiamen University, Xiamen, Fujian 361102, PR China
[b] Fujian Collaborative Innovation Center for Exploitation and Utilization of Marine Biological Resources, Xiamen University, Xiamen, Fujian 361102, PR China
[c] State-Province Joint Engineering Laboratory of Marine Bioproducts and Technology, Xiamen University, Xiamen, Fujian 361005, PR China

ARTICLE INFO

Article history:
Received 20 February 2017
Received in revised form
1 May 2017
Accepted 5 June 2017

Keywords:
Antimicrobial peptide
Sph_{12-38}
Antimicrobial activity
Oryzias melastigma
Aeromonas sobria

ABSTRACT

Antimicrobial peptides (AMPs) represent an efficient part of innate immunity and are found in a variety of life. Among them Histone 2A (H2A), as a promising class of AMPs, attracts great attention, but the *in vivo* mechanism of H2A derived AMP is still less known. Based on the acquisition of Sphistin, a synthetic 38-amino acid H2A derived peptide from *Scylla paramamosain*, as reported in our previous study, was truncated into three short fragments (Sph_{12-38}, Sph_{20-38} and Sph_{30-38}) and further investigated for its possible functional domains. The antimicrobial activities of these analogs against different Gram-positive bacteria, Gram-negative bacteria and fungi were illustrated. Among the analogs, Sph_{12-38} showed a stronger activity with a much lower minimum inhibitory concentration (3 μM) against *Staphylococcus aureus, Corynebacterium glutamicum, Micrococcus lysodeikticus* Fleming, *Bacillus subtilis, Pseudomonas fluorescens, Aeromonas hydrophila* and *A. sobria* in comparison with the reported Sphistin. A leakage of intracellular content was described in *E. coli* treated with Sph_{12-38}. Unlike Sphistin which mainly disrupts the membrane integrity, Sph_{12-38} could also combine the *A. sobria* genomic DNA with a minimum concentration of 6 μM and was located intracellularly in cells observed under confocal laser scanning microscope imaging. In comparison with the control group of *Oryzias melastigma* injected with *A. sobria* alone, the group treated with a mixture of Sph_{12-38} and *A. sobria* showed a higher survival rate 7 days post-injection. Furthermore, in a pretreatment assay at 6 h, a higher survival rate was observed in the group injected with the mixture of Sph_{12-38} and *A. sobria*. Taken together, the synthetic peptide of Sph_{12-38} had a potent antimicrobial activity against bacteria. However, Sph_{12-38} had no cytotoxicity towards the hemolymph of *S. paramamosain*. Our study suggested that, as with Sph_{12-38}, the H2A derived peptides were more likely prone to exert their activities *in vivo* through the truncated fragments while defending against different species of pathogens.

1. Introduction

Antimicrobial peptides (AMPs) are important components of innate immune defense, exerting indispensable roles against exogenous pathogen invasion. In regard to this, AMPs from different species have been studied in terms of their potential application as pharmaceuticals used in medicine and aquaculture [1,2]. However, not all AMPs are easily and effectively expressed in *Escherichia coli* or *Pichia pastoris* in order to obtain a large quantity of biologically active product, since some AMPs with long sequences show toxicity against normal cells [3]. Therefore, to solve this defect, researchers have attempted to truncate AMPs into several fragments and to use these truncated analogs as therapeutic agents [4–6].

Histones are considered as a promising type of AMP and, traditionally, are well known to be structural supports for DNA and regulators of gene transcriptions [7]. Over time, new biological roles of histones such as involvement in apoptosis [8], as a pattern recognition receptor for LPS [9], participation in the formation of

* Corresponding author. State Key Laboratory of Marine Environmental Science, College of Ocean & Earth Science, Xiamen University, Xiamen, Fujian 361102, PR China.
E-mail address: wkjian@xmu.edu.cn (K.-J. Wang).

http://dx.doi.org/10.1016/j.fsi.2017.06.013
1050-4648/

extracellular traps [10] and involvement in host defense systems [11] are continuously reported. In addition, many histone varieties are also shown to exhibit remarkable antimicrobial properties [12,13]. Already, several AMPs derived from histones, such as parasin I [14], buforin I [15] and abhisin [16] are well studied. Many histone-derived AMPs are isolated and characterized from natural sources. Buforin I, isolated from the stomach of *Bufo bufo gargarizans*, is derived from the N-terminal region of histone 2A (H2A) and shows potent antimicrobial activities against fungi and Gram-positive and Gram-negative bacteria [15]. Parasin I was first isolated from the epithelial mucosal layer of catfish and presents a broad-spectrum antimicrobial activity against different Gram-positive and Gram-negative bacteria [14]. In addition, hipposin, which is a novel 51-residue AMP isolated from the skin mucus of Atlantic halibut, has a sequence showing similarity with those of buforin I and parasin I [17].

At present, two antimicrobial modes have been revealed for these reported histone derived AMPs. One mode of antimicrobial mechanism is to change the membrane permeability to dig holes in the cell membranes. Like hipposin [17], buforin I [15] and parasin [14], these AMPs kill bacteria by inducing membrane permeabilization. Another antimicrobial mode of the histone derived AMPs shows direct entrance into bacteria without changing membrane permeability. This type of AMP can cross the target cell membrane by transition, and influence the basic cellular processes, such as protein synthesis, nucleotide synthesis, enzyme activity, cell wall formation and so on [18]. One good example is buforin II [19], which kills the bacteria mostly through targeting intracellular substance unlike the normal case in α-helical AMPs which plays its role mainly by destroying the membrane integrity.

As well as their discovery in mammals [20], histone derived AMPs are also extracted from marine animals such as the catfish *Parasilurus asotus* [21], Pacific white shrimp *Litopenaeus vannamei* [12], scallop *Chlamys farreri* [22] and black water oyster *Crassostrea madrasensis* [23]. However, information on histone derived AMPs from *Scylla paramamosain* is scarce. The newly discovered peptide Sphistin is recently reported [24]. It has significant similarity in amino acids with several known histone derived AMPs such as buforin I, hipposin and abhisin, and acts against bacteria through permeabilization of the bacterial cell membranes rather than penetrating the cell membrane.

In our study, based on the amino acid sequence of Sphistin, we synthesized three fragments of Sphistin. The antimicrobial activity of each designed analog was investigated using several assays including the confocal microscopic imaging of the action site. The *in vivo* activity of the three fragments was also investigated using medaka challenged with a live bacterium. The cytotoxicity assay was in parallel performed to measure whether these truncated fragments of Sphistin were toxic to the normal crab hemolymph and the cultured HeLa cells.

2. Materials and methods

2.1. Design and synthesis of Sphistin analogs

The structure of peptide Sphistin was predicted on the Protein Structure Prediction Server (http://www.biologydir.com/protein-structure-prediction-server-psipred-info-1758.html). There were two α-helixes (residues 12–23 and 30–35) flanked by coil regions (residues 1–11, 24–29 and 36–38) in the Sphistin secondary structure. Between the two α-helixes, a proline hinge might exist. Then Sphistin was truncated from the N-terminal coil region to residues 12 to 38 (Sph_{12-38}), 20 to 38 (Sph_{20-38}) and 30 to 38 (Sph_{30-38}) to evaluate the contribution of antimicrobial activity of the helical regions. Sphistin and its three analogs were commercially synthesized to >90% purity by Invitrogen (Shanghai, China). The amino acid sequences of Sphistin analogs are listed in Table 1.

2.2. Antimicrobial assay

Antimicrobial activity was determined using the minimum inhibitory concentration (MIC) values [25]. Briefly, synthetic Sphistin and its analogs were diluted to final concentrations from 1.5 μM to 96 μM with Milli-Q sterilized water. The microorganisms were diluted with 10 mM phosphate buffer (PBS, pH 7.4) to 3.3×10^4 cfu/mL and incubated with serial dilutions of truncated peptides. Samples without peptides were considered as blanks. After 20 h (40 h for yeast) of incubation at 30 °C, the MIC at which the lowest concentration of peptide inhibiting growth of the organisms was determined. Then the cultures were plated on appropriate agar and the minimum bactericidal concentration (MBC) value, which is the least concentration showing no bacterial growth after incubation at room temperature for 24 h–48 h, was recorded. All the values were averaged using three independent measurements (Table 2).

2.3. Kinetics of bacterial killing

Based on the MIC and MBC results above, an evaluation of killing kinetics [26] was performed using Aeromonas sobria incubated with truncated fragment of Sph_{12-38}. Synthetic Sph_{12-38} at a concentration of 1 × respective MBC (12 μM) was performed and the procedure was generally the same as mentioned for antimicrobial assay. Aliquots of 6 μL of peptide and bacteria mixtures were removed at various intervals (15 and 30 min, 1, 2, 4 and 6 h) and diluted with 10 mM PBS (pH 7.4) onto nutrition broth agar. After overnight incubation at 30 °C, the recovered colonies were counted. Each assay was repeated three times.

2.4. Membrane integrity assay

In order to examine the Sph_{12-38} peptide's interference with bacteria, an assay of real-time membrane integrity was performed. The modified *E. coli* (MC1061) constitutively expresses recombinant luciferase [27]. When perforation of the plasma membrane occurred, the externally added D-luciferin (Sigma) flooded in and caused the emission of light. Briefly, 50 μL of MH medium was mixed with 2 mM D-luciferin (10 mM Tris-HCl buffer, pH 7.4) and 1×10^7 CFU of *E. coli* cells (MC1061). Then, we diluted the mixture with 50 μL Sph_{12-38} peptide dilution to different final concentrations (6, 25 and 50 μM). Cecropin P1 and Argireline (Invitrogen) were used as positive and negative controls. The fluorescence signal was captured using TECAN Infinity microplate reader (Tecan, USA). All assays were repeated at least three times.

2.5. DNA gel mobility shift assay

The DNA binding affinity experiment was conducted with some modification based on a previous study [28]. The *A. sobria* genome

Table 1
Amino acid sequences of different antimicrobial peptides.

Name	Amino acid sequence (N→C)
Sph_{12-38}	KAKAKAVSRSARAGLQFPVGRIHRHLK
Sph_{20-38}	RSARAGLQFPVGRIHRHLK
Sph_{30-38}	VGRIHRHLK
Sphistin	MAGGKAGKDSGKAKAKAVSRSARAGLQFPVGRIHRHLK
buforin II	TRSSRAGLQFPVGRVHRLLRK
parasin I	KGRGKQGGKVRAKAKTRSS

Table 2
Minimal inhibitory concentrations (MIC) and minimum bactericidal concentration (MBC) of Sphistin and its analogs.

Microorganisms	Sphistin		Sph_{12-38}		Sph_{20-38}		Sph_{30-38}	
	MIC	MBC	MIC	MBC	MIC	MBC	MIC	MBC
Gram-positive bacteria								
Micrococcus lysodeikticus Fleming	1.5–3	6	0.75–1.5	3	3–6	12	>48	>48
Micrococcus luteus	0.75–1.5	6	0.75–1.5	1.5	1.5–3	3	6–12	6
Staphylococcus aureus	0.75–1.5	3	1.5–3	3	3–6	12	12–24	24
Bacillus subtilis	1.5–3	3	1.5–3	3	3–6	6	>48	>48
Corynebacterium glutamicum	0.75–1.5	3	0.75–1.5	3	1.5–3	12	12–24	>48
Staphylococcus epidermidis	3–6	12	1.5–3	3	12–24	48	>48	>48
Gram-negative bacteria								
Pseudomonas fluorescens	1.5–3	3	0.75–1.5	6	3–6	12	6–12	48
Shigella flexneri	1.5–3	12	0.75–1.5	3	3–6	24	>48	>48
Pseudomonas stutzeri	0.75–1.5	3	0.75–1.5	6	3–6	12	>48	>48
Aeromonas hydrophila subsp. *hydrophila*	0.75–1.5	3	0.75–1.5	3	3–6	24	>48	>48
Escherichia coli	1.5–3	24	1.5–3	24	3–6	48	>48	>48
Aeromonas sobria	>48	>48	3–6	12	>48	>48	>48	>48
Edwardsiella tarda	>48	>48	>48	>48	>48	>48	>48	>48
Vibrio parahaemolyticus	>48	>48	>48	>48	>48	>48	>48	>48
Vibrio alginolyticus	>48	>48	>48	>48	>48	>48	>48	>48
Vibrio harveyi	>48	>48	>48	>48	>48	>48	>48	>48
Vibrio fluvialis	>48	>48	>48	>48	>48	>48	>48	>48
Yeast								
Pichia pastoris GS115	6–12	24	6–12	12	6–12	12	12–24	48
Candida albicans	24–48	>48	24–48	>48	>48	>48	>48	>48

DNA was extracted using a TIANamp Bacteria DNA Kit (Tiangen, China). Sph_{12-38} peptide and Argireline were diluted to increasing final concentrations (0, 6, 12, 24, 48, 72 and 96 μM) in 40 μL of Tris-HCL buffer. Then we incubated the peptide dilution with 350 ng *A. sobria* genome DNA at room temperature for 30 min. After adding loading buffer, the DNA migration was assessed using 0.8% agarose gel electrophoresis and detected using Dured fluorescence. We reformed Argireline as the negative control peptide.

2.6. Confocal microscopy imaging of A. sobria

To further investigate the antimicrobial mechanism of Sph_{12-38} peptide, we used two-photon confocal microscopy to detect its action site. The A. sobria bacterial suspension was washed with 10 mM PBS (pH 7.4) and diluted to 5×10^7 cfu/mL. The FITC-labeled Sph_{12-38}, buforin II and Argireline (Bioss, China) were diluted with Milli-Q water to 800 μg/mL. Then bacterial suspension and each peptide dilution were mixed in equal quantity and incubated at room temperature for 1 h. Next, we immobilized the suspension in 200 μL of 4% paraformaldehyde for 20 min. After washing the mixture of *A. sobria* and Sph_{12-38} three times with 10 mM PBS (pH 7.4), the suspension was dropped on a polylysine slide for 30 min at 4 °C before the slide was washed another twice and then covered with 0.5 μg/mL DAPI fluorescence for 15 min protecting it from light. After washing the glass slide three times with PBS (pH 7.4), the action site of the labeled peptide and bacteria was observed under a multiphoton confocal LSM 780 NLO microscope (Carl Zeiss, Germany). DNA is stained with DAPI (blue) and FITC-labeled Sph_{12-38} is green under 488 nm excitation.

2.7. Sph_{12-38} and bacterial challenge of medaka

To determine the 50% lethal dose, 10 groups of mature 15 medaka, which weighed 0.23 g in average, were intraperitoneally injected with *A. sobria* (to final concentrations of 1×10^7, 5×10^6, 1×10^6, 5×10^5, 2×10^5, 1×10^5, 5×10^4, 2×10^4, 1×10^4 and 1×10^3 cfu/fish). For the control group, only saline was injected. Mortality of medaka was recorded at 3, 6, 12, 24, 36, 48, 60 and 72 h (data not shown).

To test the protective role of Sph_{12-38} *in vivo*, we conducted two trials. For the first trial, 150 mature medaka fish were used and separated equally into five groups. The peptide of Sph_{12-38} was reconstituted in saline (pH = 7.4) for the experiment. Group 1 was injected with 5×10^4 cfu/fish of *A. sobria* and saline; and Groups 2 to 4 were injected with 5×10^4 cfu/fish of *A. sobria* mixed with different final amounts (1, 5 and 10 μg/fish) of Sph_{12-38}. Group 5 was injected with only saline and considered as a control group. The mortality rate was recorded after 3, 6 and 12 h, and then on a daily basis for 1 week.

For the second trial, there were six groups, each containing 15 mature fish. The fish in groups 1 and 2 were firstly injected with 5 μg/fish Sph_{12-38}, then, after 3 or 6 h, 5×10^4 cfu/fish of *A. sobria* was injected. The mortality rate was recorded after 3, 6 and 12 h, and then on a daily basis for 1 week. In Groups 3 and 4, each fish was injected firstly with saline and then, after 3 or 6 h, with 5×10^4 cfu/fish of *A. sobria*. In Groups 5 and 6, saline was injected into each fish and after 3 or 6 h reinjected again. The mortality rate was recorded after 3, 6 and 12 h, and then on a daily basis for 1 week.

2.8. Real-time PCR

The immune associated genes expression profiles were detected using qPCR. 15 mature medaka were injected with 5 μg/fish peptides of Sphistin and 15 with Sph_{12-38}. Another 15 fish were injected with a mixture of Sph_{12-38} peptide (5 μg/fish) and *A. sobria* (1×10^4 cfu/fish), and a further 15 with a mixture of Sphistin peptide (5 μg/fish) and *A. sobria* (1×10^4 cfu/fish). A group of 15 medaka injected with only *A. sobria* (1×10^4 cfu/fish) was treated as the positive control, while another group of 15 medaka injected with only saline was the negative control. The kidneys of three fish in each group were collected at 3, 6, 12, 24 and 48 h after treatment. Trizol reagent (Invitrogen) was used for RNA extraction. The RNA isolation and the cDNA synthesis were performed following the manufacturer's instructions. Real-time PCR was performed on an ABI Prism 7500 instrument (Applied Biosystems) under the conditions: 2 min at 50 °C, 10 min at 95 °C, 40 cycles of 15 s at 95 °C then 1 min at 60 °C. The housekeeping gene 16S was used to normalize the relative quantities. All assays were repeated at least

three times. All the immune associated genes used in the present study were selected from medaka transcriptome data (not yet published). The sequences of primers are listed in Table 3.

2.9. Cytotoxicity assay

Cell cytotoxicity was determined on human cervical tumor HeLa cells and measured using 3-(4,5-dimethylthiazol-2-yl)-5-(3-carboxymethoxyphenyl)-2-(4-sulfophenyl)-2H-tetrazolium (MTS) according to the instruction of CellTiter 96®AQueous Non-Radioactive Cell Proliferation assay (Promega, USA). 100 μL of HeLa cells were seeded in 96-well plates at 10^4 cells/well and incubated in DMEM (Life Technologies) supplemented with 10% FBS, 100 μg/mL penicillin and 100 U/mL streptomycin at 37 °C under 5% CO_2. Then the cells were treated with different concentrations of Sph_{12-38} (0, 0.034, 0.34, 3.4 and 34 μM) for 24 h. After that, the HeLa cells were placed under an inverted Leica DMIRB microscope and their morphology photographed. The cells were treated with 20 μL MTS solution for another 6 h, and then absorbance values at 490 nm were made on a microplate reader (Tecan, USA). Each assay had at least three independent experiments.

3. Results

3.1. Sph_{12-38} shows high antimicrobial activity against microorganisms

The antimicrobial activities of Sphistin and its analogs are listed in Table 2. In the study, 19 microorganisms were used, including Gram-positive bacteria, Gram-negative bacteria and yeast. Generally, Sphistin, Sph_{12-38} and Sph_{20-38} all could effectively inhibit the growth of the Gram-positive bacteria (*Micrococcus lysodeikticus* Fleming, *M. luteus*, *S. aureus, Bacillus subtilis* and *Corynebacterium glutamicum*) and Gram-negative bacteria (*Pseudomonas fluorescens, Shigella flexneri, P. stutzeri, Aeromonas hydrophila* subsp. *hydrophila* and *E. coli*), while Sphistin and Sph_{12-38} showed a more potent activity than Sph_{20-38}. However, the antimicrobial activity of Sph_{30-38} against all the detected microorganisms was not significant. Sph_{12-38} was the only peptide that potently inhibited the growth of *A. sobria*. Aquaculture pathogenic bacteria of *A. hydrophila*, zoonosis pathogen of *S. aureus* and *S. epidermidis* could also be significantly inhibited by Sph_{12-38}. This suggested a broad spectrum of antimicrobial activity for Sph_{12-38}.

In general, Sph_{12-38} exhibited greater antimicrobial activity than the other designed analogs. Additionally, Sph_{12-38} showed similar activity as Sphistin in most of the microorganisms tested, and was much stronger than Sphistin against *A. sobria*.

To further investigate how rapidly *A. sobria* was killed by Sph_{12-38}, the killing kinetics of Sph_{12-38} were subsequently measured (Fig. 1). Approximately 60% killing of *A. sobria* was achieved in 30 min. Meanwhile, it took totally 6 h to kill 100% of the strains. This revealed a rapid bactericidal kinetics effect of Sph_{12-38} against *A. sobria*.

3.2. Sph_{12-38} causes the permeabilization of bacteria membrane

To examine whether or not Sph_{12-38} killed bacteria through destroying membrane integrity, a membrane integrity assay was carried out (Fig. 2). Result showed that, after adding 50 μM Sph_{12-38}, a strong peak of light emission was observed, which was even stronger than cecropin P1. Cecropin P1 is well studied for killing bacteria by inserting pores into membranes, and was used as the positive control in our study. When modified *E. coli* was exposed to cecropin P1, a strong fluorescence signal was observed. No light emission was detected when Argireline was present, so it served as the negative control. Under treatment of 25 μM Sph_{12-38}, a peak of light emission could also be captured but weaker than at 50 μM. This result indicated that Sph_{12-38} might affect cell membrane integrity by disturbing its permeability, thus leading to bacteria killed.

Table 3
The primers synthesized for genes amplification by PCR.

Primers	Sequence (5′-3′)
16S-F	CATAAGACGAGAAGACCCTGTGGAGC
16S-R	GCGGTCGCCCCAACCAAAGACACTA
IL8-F	TGCGCTGTCTTCTTGGGCTT
IL8-R	CCTTCTGAATGTGGCGCCCG
TLR5-F	CCTGTCCTCCAACGCCCTGA
TLR5-R	TGGAGAGACCCACGACGCTG
TNFR-1-F	ACCTGGACGACCGCTGACTC
TNFR-1-R	TGCCCTGACACCGCTCAACT
TNIP1-F	CGACGGGGTGTGAAGGTTTA
TNIP1-R	CAGACAACGACTGGCTGAGT
TNIP2-F	GGCTAGGGCGGTACGAGAGG
TNIP2-R	CCGGCTGACACCGGACTCTT
TANK-F	CCAACTCCTGGAAGGGGCCA
TANK-R	TGGGCATGGAGAACCGCTGA
PDE4-F	CTGTACCGGCAGTGGACGGA
PDE4-R	TGCCCACGTCTCCCACAGAG
STAT3-F	CGCCCTGGAAGAGAAGATTGTGGAT
STAT3-R	CCAGCAACCTGACTTTGTTTGTGAA

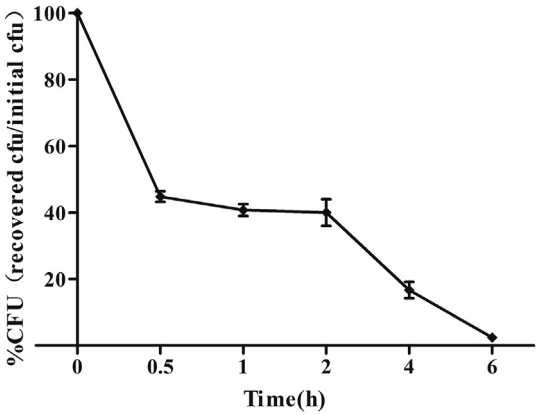

Fig. 1. Kinetics of the bacterial activity of Sph_{12-38} peptide against *A. sobria*. 12 μM of peptide Sph_{12-38} was incubated with *A. sobria*. The recovered bacterial colonies were counted at 15 and 30 min, 1, 2, 4 and 6 h after incubation.

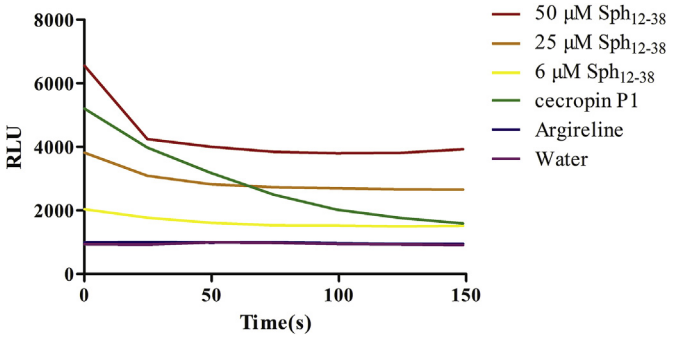

Fig. 2. Effect on bacterial membrane integrity by Sph_{12-38} at different concentrations. Light emission kinetics of *E. coli* (MC1061) cells were treated with Sph_{12-38}. Light emitted after adding 6 μM Sph_{12-38}, 25 μM Sph_{12-38}, 50 μM Sph_{12-38}, 50 μM Argrieline and 1 μM cecropin P1.

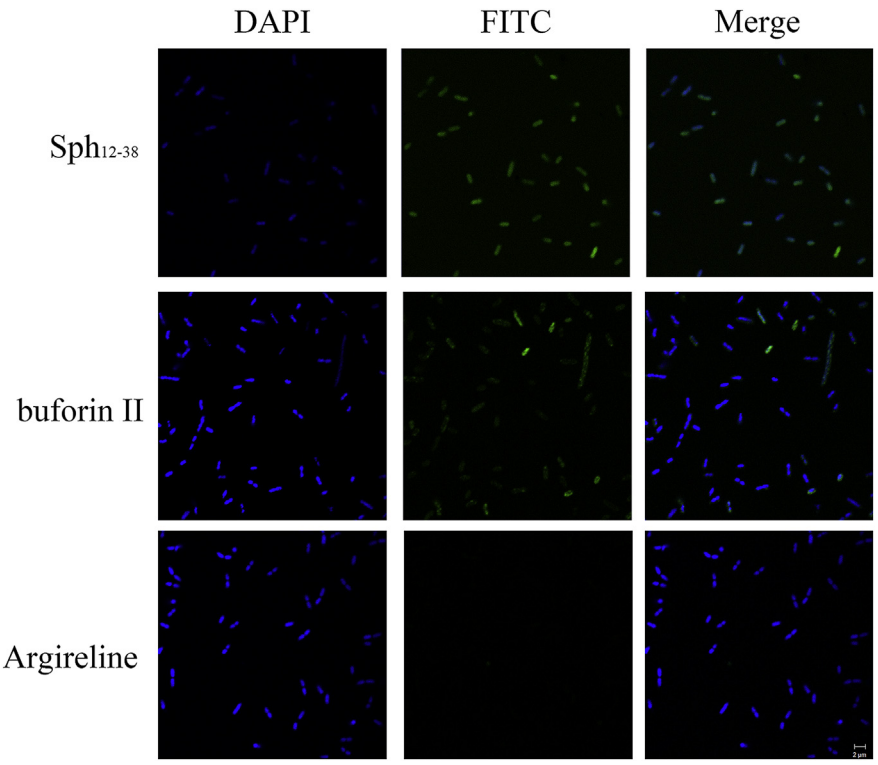

Fig. 3. Localization of Sph_{12-38} in *A. sobria* as examined using confocal laser scanning microscopy. *A. sobria* cells were treated with Sph_{12-38}. Fluorescence of DAPI, FITC-labeled Sph_{12-38}, as well as merged images, is presented. DAPI attached to DNA (blue) and FITC-labeled Sph_{12-38} (green). (For interpretation of the references to colour in this figure legend, the reader is referred to the web version of this article.)

3.3. Sph_{12-38} locates inside the bacteria cells

To examine the localization of the action site of Sph_{12-38}, confocal microscopy imaging was performed after incubation with *A. sobria* (Fig. 3). We labeled FITC fluorescence to the N-terminal of Sph_{12-38} in order to detect its action site. The fluorescence of DAPI strongly combined with bacterial DNA and emitted blue light under UV radiation. The image suggested that the action site of Sph_{12-38} was internalized in the cell. Buforin II served as the positive control which killed bacteria by penetrating the membrane. We observed a similar imaging of buforin II with $Sph_{12-38\ in}$ which blue and green fluorescence overlapped with each other. On the other hand, in the image of negative control peptide Argireline we observed only blue fluorescence. This is indicated that Sph_{12-38} might bind to DNA and share the same antimicrobial mechanism as buforin II.

3.4. Sph_{12-38} binds to A. sobria genome DNA

The affinity of Sph_{12-38} with the genomic DNA of *A. sobria* was observed using the gel mobility shift assay. When the quantity of Sph_{12-38} increased to be 6 μM, a band signaling the genomic DNA of *A. sobria* incubated with this peptide appeared to shift slower than the sample with DNA only. As the amount of Sph_{12-38} product increased, the incubation of peptide and genomic DNA of *A. sobria* was gradually retarded at the gel hole. Comparatively, the control of Argireline product incubated with the genomic DNA of *A. sobria* did not show any retardation (Fig. 4).

3.5. Sph_{12-38} exhibits antimicrobial property after co-treatment

To determine the proper injected dose of *A. sobria* using in our

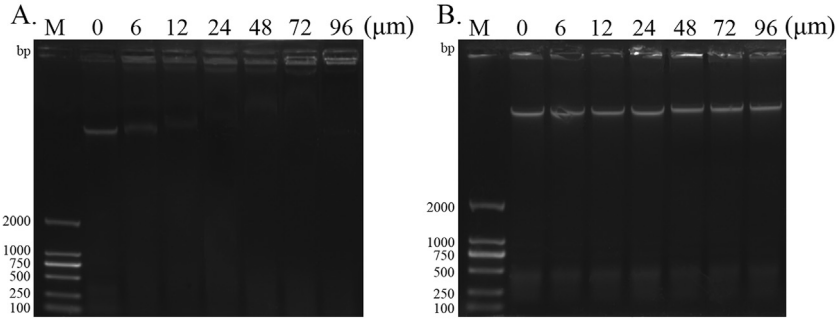

Fig. 4. The DNA binding affinity of Sph_{12-38} peptide to *A. sobria* DNA. Various amounts (0–96 μM) of peptide Sph_{12-38} and peptide Argireline (considered as the control) were incubated with 350 ng *A. sobria* DNA. A: peptide Sph_{12-38} with *A. sobria* DNA, B: peptide Argireline with *A. sobria* DNA, M: *DS*2000™ DNA marker.

study, different doses of *A. sobria* were intraperitoneally injected into medaka, and at between 10^4 and 10^5 cfu/fish the survival rate significantly decreased. Under the dosage of 5×10^4 cfu/fish, the mortality reached about 50% and stayed stable. Therefore, we chose this dose to perform the co-treatment experiment.

Mature medaka were injected with different doses of synthetic Sph_{12-38} peptide and live 5×10^4 cfu/fish *A. sobria* at the same time. As shown in Fig. 5A, high mortality occurred 1 day after bacterial challenge: the medaka injected with 5 μg/fish and 10 μg/fish of Sph_{12-38} reached an 80% survival rate in contrast to the group injected with *A. sobria* only. These data suggested that Sph_{12-38} could protect medaka from *A. sobria* attack *in vivo* and enhance the survival rate.

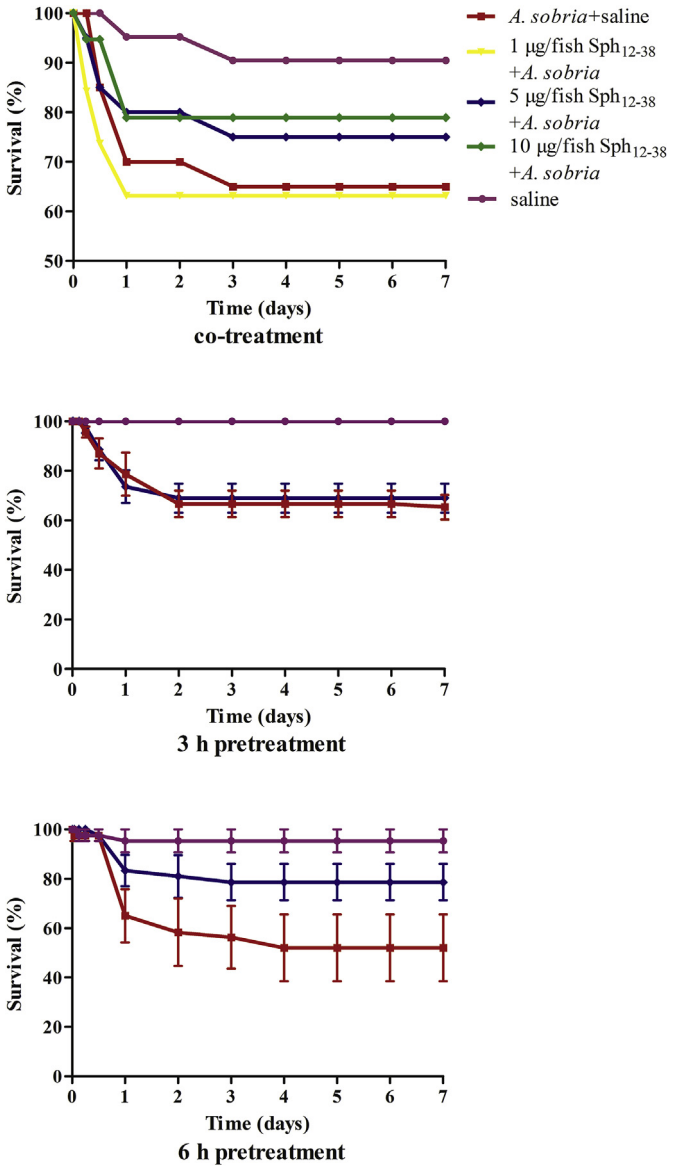

Fig. 5. A. The survival rate of medaka after being co-injected with *A. sobria* and Sph_{12-38}. Cumulative survival rates of medaka co-injected with Sph_{12-38} (1, 5 and 10 μg/fish) or saline and *A. sobria* (5×10^4 cfu/fish) were measured. The mortality was recorded for 7 days after the bacterial challenge. **B.** The survival rate of medaka injected with Sph_{12-38}, or saline, and 3 h later *A. sobria*. 15 medaka were first injected with Sph_{12-38} (5 μg/fish) and 15 with saline, followed by injection with *A. sobria* (5×10^4 cfu/fish) 3 h later. The mortality was recorded for 7 days after the bacterial challenge. Each bar represents the mean value from three determinations with the standard error. **C.** The survival rate of medaka injected with Sph_{12-38} or saline, and 6 h later *A. sobria*. 15 medaka were first injected with Sph_{12-38} (5 μg/fish) and 15 with saline, followed 6 h later by injection with *A. sobria* (5×10^4 cfu/fish). The mortality was recorded for 7 days after the bacterial challenge. Each bar represents the mean value from three determinations with the standard error.

3.6. Sph_{12-38} exhibits antimicrobial property after pretreatment

To determine the antimicrobial protective activities of Sph_{12-38}, pretreated groups were first injected with Sph_{12-38} and then injected with *A. sobria* at different time intervals. As shown in Fig. 5B, after 3 h of treatment with Sph_{12-38}, the survival rate was closely similar to the group injected with saline and *A. sobria*. High mortality occurred 12–36 h after the bacterial challenge and, at 2 days after challenge, the survival rates of the Sph_{12-38} injected group and without Sph_{12-38} injected group were 69% and 65%, respectively. The fish in the group injected with saline rarely had any deaths. However, as shown in Fig. 5C, the fish exhibited a survival rate of 79% in the group with a 6 h pretreatment injection of Sph_{12-38} compared with a survival rate of 52% in the group without pretreatment 7 days post injection.

3.7. Sph_{12-38} modulates immune associated genes expression

To investigate the immune response of Sph_{12-38} against *A. sobria* infection, the expression level of several immune associated genes were measured using real-time PCR (Fig. 6). At first we carried out a pre-experiment. The tested fish were injected with *A. sobria*, then the mRNA expression of seventeen immune associated genes used in the study were detected and we found eight among the tested genes were significantly expressed. Thus, the eight genes were selected to be further used in the following experiment. Then the experiment was carried out using a mixture of Sph_{12-38} and *A. sobria* injected into fish and then the mRNA expressions of the eight immune-associated genes were tested. The expression levels of NF-κB negative regulators such as of TNIP1 and TNIP2 [29] in fish injected with a mixture of Sph_{12-38} and *A. sobria* significantly declined compared with fish injected with *A. sobria* alone after 3, 6 and 12 h treatment, so as the TRAF family member-associated NF-κB activator (TANK) [30]. The transcription levels of Interleukin (IL) 8 [31], a pro-inflammatory CXC chemokine, had an obvious decline at 3 and 12 h in the Sph_{12-38} and *A. sobria* treatment. Meanwhile, phosphodiesterases 4 (PDE4) [32] which is the dominant PDE in inflammatory cells was also observed declines at 3 and 12 h. STAT3 [33] involved in JAK/STAT3 pathway showed a decline at 12 h while Tumor necrosis factor receptor-1 (TNFR-1) [34] presented a lower expression level at 24 h after injection with Sph_{12-38} and *A. sobria*. Toll signaling pathway associated gene TLR5 [35] transcript amount was significantly lower 3 h after injection with Sph_{12-38} and *A. sobria* compared with that injected only with *A. sobria*. Results indicated that Sph_{12-38} might reduce the inflammatory response caused by the challenge of *A. sobria*. However, the fish injected only with Sph_{12-38} had no significant difference compared with the fish in the saline group. This suggested that Sph_{12-38} might be a safe foreign protein and less effect on the immune response of medaka *in vivo*.

3.8. Sph_{12-38} exhibits no cytotoxicity on HeLa cells and crab hemolymph

Along with the dose of Sph_{12-38} increased, the morphology of HeLa cell and crab hemolymph did not change. Through MTS assay (Fig. 7), we detected the relative amount of living cells and cell activity. We analyzed the MTS solution processed cell using microplating and the results revealed that the viability of the cells was not severely different. This suggested that Sph_{12-38} would not

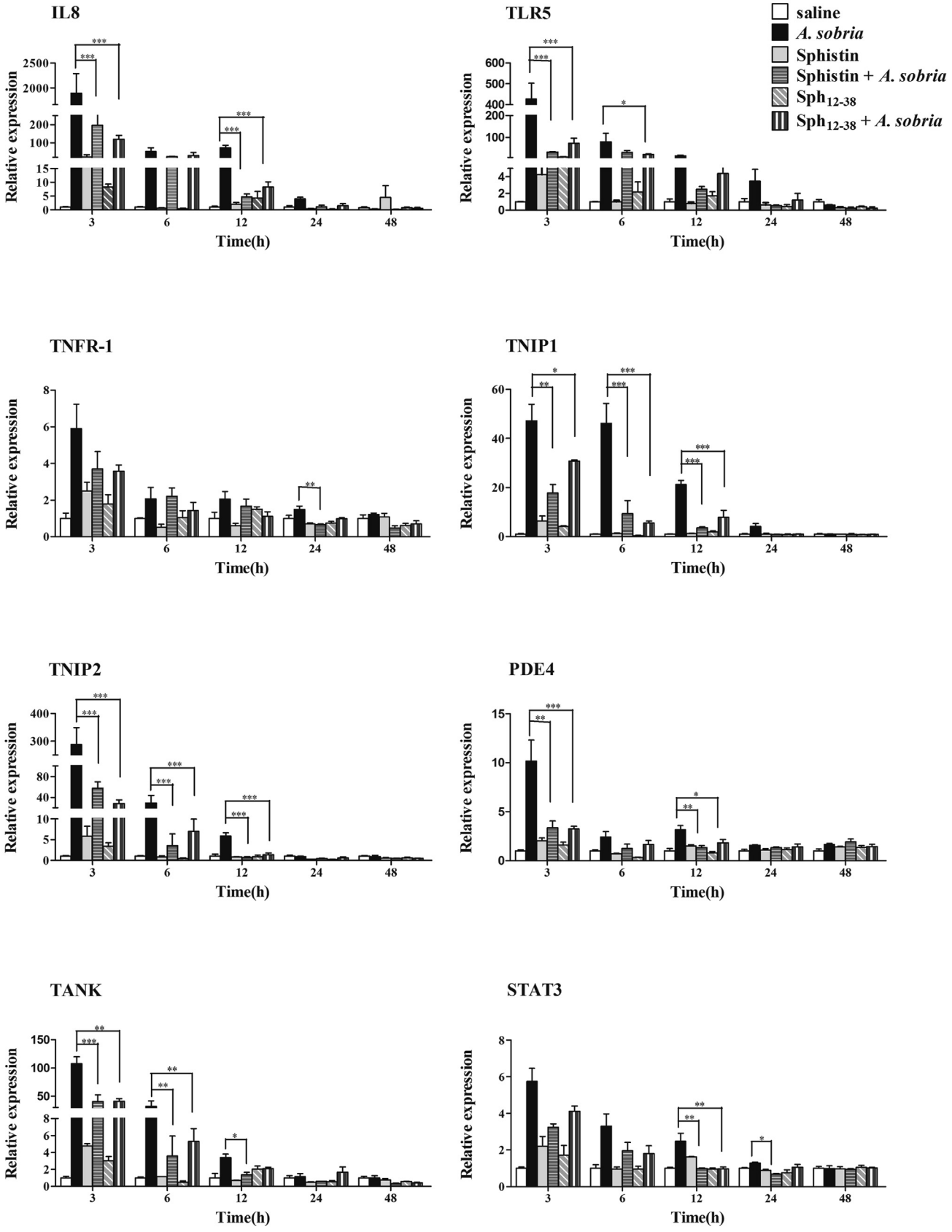

Fig. 6. The relative expression of immune associated genes (IL8, TLR5, TNFR-1, TNIP1, TNIP2, PDE4, TANK and STAT3) in medaka after injection with *A. sobria* and Sph_{12-38}. Relative expressions of immune associated genes were normalized via the expression of housekeeping gene 16s. Samples were collected at 3, 6, 12, 24 and 48 h. Each bar represents the mean value from three determinations with the standard error. Measurements were significantly different from the control group at $P < 0.05$ (*), $P < 0.01$ (**) and $P < 0.001$ (***).

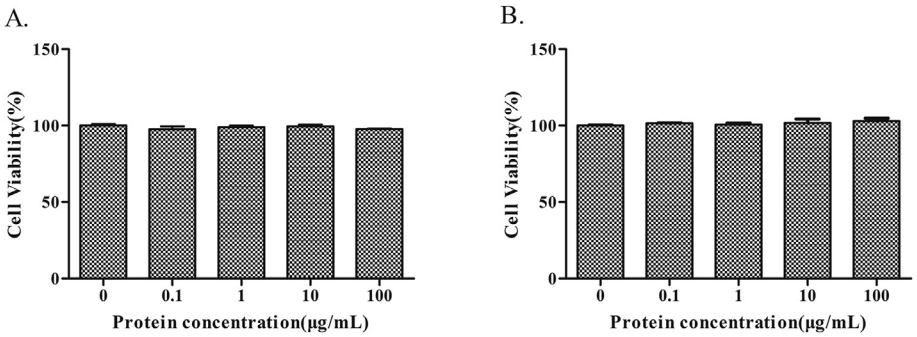

Fig. 7. MTS assay of the effect of Sph_{12-38} on the cell viability of hemocytes from *S. paramamosain* and HeLa. HeLa cells (A) and hemocytes from *S. paramamosain* (B) were incubated with Sph_{12-38} peptide (0, 0.034, 0.34, 3.4 and 34 μM) at 37 °C and 20 °C, respectively. Cell viability is represented as the percentage relative to the control. ($P < 0.05$, one way ANOVA followed by Tukey's post hoc test).

lead to the death of cells and had no obvious toxicity towards HeLa cells or the normal hemocyte of *S. paramamosain*.

4. Discussion

So far, the *in vivo* mechanism of an AMP has been relatively less revealed than its *in vitro* activities. Some AMPs are reported to exert their roles with a truncated fragment. Buforin II, a 21-amino acid AMP derived from buforin I displays a higher antimicrobial activity level than buforin I [36]. The N-terminal fragments of histone H1 and H2B identified in the skin mucus of the Atlantic salmon (*Salmo salar*) [6] and in human wounds [5] have broad-spectrum antimicrobial properties. Sphistin, a 38-amino acid peptide synthesized based on the sequence of H2A cloned from *S. paramamosain*, shows a potent activity against several bacterial species reported in our previous study [24]. In the present study, the synthesized truncated fragment of Sph_{12-38} presented a somewhat different antimicrobial mechanism and a higher antimicrobial activity level in comparison with the intact Sphistin. In view of those observations, a query is raised whether a peptide would be prone to degrade into one or several fragments automatically to play a role against various exogenous pathogens and/or meet the requirements of defending the possible multiple infectious routes of pathogens into a host. Thus, we presumed that there might be a natural morphological structure existing *in vivo* in the mud crab such as a degraded fragment of Sphistin to exert its activity against invading bacteria. As a vital immune associated component, H2A derived AMPs might have the predicted multiforms to exert activities against various microorganisms *in vivo*.

Several studies reveal discrepancies in the antimicrobial activity among the histone derived peptides and their truncated analogs [19,37]. In the present study, the antimicrobial activities of different Sphistin analogs were dramatically dissimilar. Sph_{12-38} was the only analog among the three fragments which had an obvious inhibition function on *A. sobria* and showed a higher antimicrobial activity compared with Sphistin. It was noted that the residues 12–38 of the Sphistin sequence contained both an α-helix and proline hinge. As is known, the α-helix structure of AMPs is usually involved in antimicrobial function and one AMP with more α-helix structures is thought to be a better AMP. In addition, the proline hinges between α-helix structures also work as a vital factor in antimicrobial activity [38–40] and the replacement of hinge amino acids with proline can highly improve the antimicrobial activity effect [41]. Further observation indicates that the existence of proline is directly associated with the process of AMPs penetrating into the cell membrane. Lacking proline, the AMPs do not enter into the cell such as in the case of buforin II against *E. coli* [19]. Consistent with these reported results, Sph_{12-38} contained both α-helix and proline hinges and showed potent antimicrobial activity in the damage of the cell membrane as expected. The highly potent antimicrobial activity of Sph_{12-38} against *S. aureus* would make it possible as a substitute of antibiotics in the medical industry in future.

The antimicrobial mechanism of AMP buforin II involves penetrating the bacteria and combining with intracellular nuclease [42]. It was found that Sph_{12-38} had a similar effect on the membrane integrity of bacteria and caused the leakage of intracellular content. Judging by the fluorescence signal of Sph_{12-38} concentrated inside the cell under confocal laser scanning microscopy, Sph_{12-38} might have identical loci to buforin II. The result that Sph_{12-38} could bind with *A. sobria* DNA supported our speculation that Sph_{12-38} might kill bacteria via secondary effects. The cationic AMP tachyplesin I kills bacteria not only by permeabilizing the membrane but also by damaging and interfering with intracellular targets [43]. Another peptide, Indolicidin, effectively kills bacteria by either interacting with the cell membrane or inhibiting DNA synthesis [44]. In the case of hipposin, which contains the sequence of both parasin and buforin II, hipposin kills bacteria by inducing membrane permeabilization, which is associated with the parasin sequence. Without the parasin sequence, the rest of the amino acid sequences of hipposin show more similarity to buforin II whose sequence is reported mainly for DNA binding [17]. Sphistin exerted antimicrobial activity via permeabilization of cell membranes rather than penetrating into cells, and its sequence was very similar to that of buforin I, buforin II and parasin with a few single site differences [24]. Sph_{12-38} shared a conservative region with buforin II from residue 19 to residue 38 and also had a partly identical site with parasin from residue 19 to residue 22. There was also the possibility that a part of the sequence showed similarity between parasin and Sph_{12-38}, thus leading to the result that Sph_{12-38} caused bacterial membrane permeabilization. Interestingly, deletion of the 1–12 residues of the Sphistin sequence could facilitate the capability of translocation into the cell and binding with DNA. Taken together, this suggested that Sph_{12-38} might probably have different antimicrobial mechanisms either by changing membrane permeability or conducting secondary effects such as binding the bacterial DNA, as is reported in several studies that two general mechanisms can coexist when AMPs kill bacteria [45].

In the experiment involving co-treatment of Sph_{12-38} with *A. sobria*, Sph_{12-38} could improve the survival rate of *Oryzias melastigma*. As the concentration of Sph_{12-38} increased, the survival rate of the medaka was enhanced. It was possible that the treatment using different concentrations of Sph_{12-38} with *A. sobria* led to an unequal amount of live bacteria at the beginning [46]. The high

survival rate in the group with a high concentration of Sph_{12-38} might be the reason that the live bacteria in *O. melastigma* could not propagate well after being treated with Sph_{12-38} in the initial infection. It was also interesting to note from this study that in comparison with the groups injected with Sph_{12-38} 3 h before *A. sobria* challenge, the groups injected with Sph_{12-38} 6 h before challenge could increase the survival rate of *O. melastigma*. The results suggested that the longer existence of Sph_{12-38} *in vivo* might modulate the expression of other immune-associated genes, which also conferred immunity against bacterial challenge. One previous study reports that after injection of a mixture of the AMP Pt5 and *A. hydrophila*, the immune related genes are significantly expressed compared with injection of only *A. hydrophila* in zebra fish [47]. In our study, it was found that the expression levels of anti-inflammatory factors such as IL8, STAT3 and TNFR-1 and the genes involved in a Toll-like receptor signaling pathway were significantly raised with the challenge of *A. sobria*. *A. sobria* can stimulate an inflammatory response in organisms but AMPs can regulate immune activities on the host without killing microbes [48]. We consistently found in our study that increases in the mRNA expression levels of the immune genes tested, followed by injection of a mixture of Sph_{12-38} peptide and bacterium, were lower than that in the negative group (injected only with *A. sobria*). Thus, it was indicated that this peptide had a crosstalk with some immune-associated genes that in collaboration modulated the inflammatory response.

Acknowledgments

This work was supported by a Grant (U1205123) from the National Natural Science Foundation of China (NSFC), a Grant(2014N2004) from the Fujian Science and Technology Department and a grant (201405016) from Technology Research Funds Projects of Ocean, the People's Republic of China. Prof. Matti T. Karp of Tampere University of Technology (Finland) and Dr. Chun Li of the University of Tromsø (Norway) are thanks for providing us with the *E. coli* MC1061 transferred with vector pCSS962 with the luciferase gene; and thanks to Huiyun Chen, laboratory engineering staff, for the operation and analysis of confocal microscopy imaging. Prof. I. J. Hodgkiss is thanked for his help with English.

References

[1] R.E.W. Hancock, H.G. Sahl, Antimicrobial and host-defense peptides as new anti-infective therapeutic strategies, Nat. Biotechnol. 24 (12) (2006) 1551–1557.
[2] V. Rajanbabu, J.Y. Chen, Applications of antimicrobial peptides from fish and perspectives for the future, Peptides 32 (2) (2011) 415–420.
[3] J. Johansson, G.H. Gudmundsson, M.E. Rottenber, K.D. Berndt, B. Agerberth, Conformation-dependent antibacterial activity of the naturally occurring human peptide LL-37, J. Biol. Chem. 273 (6) (1998) 3718–3724.
[4] F. Guida, M. Benincasa, S. Zahariev, M. Scocchi, F. Berti, R. Gennaro, et al., Effect of size and N-terminal residue characteristics on bacterial cell penetration and antibacterial activity of the proline-rich peptide Bac7, J. Med. Chem. 58 (3) (2015) 1195–1204.
[5] V. Krishnakumari, R. Nagaraj, N-Terminal fatty acylation of peptides spanning the cationic C-terminal segment of bovine beta-defensin-2 results in salt-resistant antibacterial activity, Biophys. Chem. 199 (2015) 25–33.
[6] C. Nagant, B. Pitts, K. Nazmi, M. Vandenbranden, J.G. Bolscher, P.S. Stewart, et al., Identification of peptides derived from the human antimicrobial peptide LL-37 active against biofilms formed by *Pseudomonas aeruginosa* using a library of truncated fragments, Antimicrob. Agents Chemother. 56 (11) (2012) 5698–5708.
[7] M.H. Parseghian, K.A. Luhrs, Beyond the walls of the nucleus: the role of histones in cellular signaling and innate immunity, Biochem. Cell Biol. 84 (4) (2006) 589–604.
[8] A. Konishi, S. Shimizu, J. Hirota, T. Takao, Y.H. Fan, Y. Matsuoka, et al., Involvement of histone H1.2 in apoptosis induced by DNA double-strand breaks, Cell 114 (6) (2003) 673–688.
[9] L.A. Augusto, P. Decottignies, M. Synguelakis, M. Nicaise, P.L. Marechal, R. Chaby, Histones: a novel class of lipopolysaccharide-binding molecules, Biochemistry 42 (3) (2003) 3929–3938.
[10] V. Brinkmann, U. Reichard, C. Goosmann, B. Fauler, Y. Uhlemann, D.S. Weiss, et al., Neutrophil extracellular traps kill bacteria, Science 303 (5663) (2004) 1532–1535.
[11] H.S. Kim, J.H. Cho, H.W. Park, H. Yoon, M.S. Kim, S.C. Kim, Endotoxin-neutralizing antimicrobial proteins of the human placenta, J. Immunol. 168 (5) (2002) 2356–2364.
[12] S.A. Patat, R.B. Carnegie, C. Kingsbury, P.S. Gross, R. Chapman, K.L. Schey, Antimicrobial activity of histones from hemocytes of the Pacific white shrimp, FEBS J. 271 (2004) 4825–4833.
[13] C.B. Park, M.S. Kim, S.C. Kim, A Novel Antimicrobial peptide from *Bufo bufo gargarizans*, Biochem. Biophys. Res. Commun. 218 (1) (1996) 408–413.
[14] J.H. Cho, I.Y. Park, H.S. Kim, W.T. Lee, M.S. Kim, S.C. Kim, Cathepsin D produces antimicrobial peptide parasin I from histone H2A in the skin mucosa of fish, FASEB J. 16 (3) (2002) 429–431.
[15] H.S. Kim, H. Yoon, I. Minn, C.B. Park, W.T. Lee, M. Zasloff, et al., Pepsin-mediated processing of the cytoplasmic histone H2A to strong antimicrobial peptide Buforin I, J. Immunol. 165 (6) (2000) 3268–3274.
[16] M. De Zoysa, C. Nikapitiya, I. Whang, J.S. Lee, J. Lee, Abhisin: a potential antimicrobial peptide derived from histone H2A of disk abalone (*Haliotis discus discus*), Fish Shellfish Immunol. 27 (5) (2009) 639–646.
[17] M.E. Bustillo, A.L. Fischer, M.A. LaBouyer, J.A. Klaips, A.C. Webb, D.E. Elmore, Modular analysis of hipposin, a histone-derived antimicrobial peptide consisting of membrane translocating and membrane permeabilizing fragments, Biochim. Biophys. Acta (BBA)-Biomembr. 1838 (2014) 2228–2233.
[18] K.A. Brogden, Antimicrobial peptides: pore formers or metabolic inhibitors in bacteria? Nat. Rev. Microbiol. 3 (3) (2005) 238–250.
[19] C.B. Park, K.S. Yi, K. Matsuzaki, M.S. Kim, S.C. Kim, Structure-activity analysis of buforin II, a histone H2A-derived antimicrobial peptide: the proline hinge is responsible for the cell-penetrating ability of buforin II, Proc. Natl. Acad. Sci. 97 (15) (2000) 8245–8250.
[20] T. Dráb, Hanzlíková E. Kračmerová, T. Černá, R. Litváková, A. Pohlová, et al., The antimicrobial action of histones in the reproductive tract of cow, Biochem. Biophys. Res. Commun. 443 (3) (2014) 987–990.
[21] I.Y. Park, C.B. Park, M.S. Kim, S.C. Kim, Parasin I, an antimicrobial peptide derived from histone H2A in the catfish, Parasilurus asotus, FEBS Lett. 437 (3) (1998) 258–262.
[22] C.H. Li, L.S. Song, J.M. Zhao, L. Zhu, H.B. Zou, H. Zhang, et al., Preliminary study on a potential antibacterial peptide derived from histone H2A in hemocytes of scallop *Chlamys farreri*, Fish Shellfish Immunol. 22 (6) (2007) 663–672.
[23] N. Sathyan, R. Philip, E.R. Chaithanya, P.R. Anil Kumar, Identification and molecular characterization of Molluskin, a histone-H2A-derived antimicrobial peptide from Molluscs, ISRN Mol. Biol. 2012 (2012) 219656.
[24] B. Chen, D.Q. Fan, K.X. Zhu, Z.G. Shan, F.Y. Chen, L. Hou, et al., Mechanism study on a new antimicrobial peptide Sphistin derived from the N-terminus of crab histone H2A identified in haemolymphs of *Scylla paramamosain*, Fish Shellfish Immunol. 47 (2) (2015) 833–846.
[25] P. Bulet, J.L. Dimarcq, C. Hetru, M. Lagueu, M. Charlet, G. Hegy, et al., A Novel inducible antibacterial peptide of *Drosophila* carries an 0-Glycosylated substitution, J. Biol. Chem. 268 (20) (1993) 14893–14897.
[26] J.M. Decazes, J.D. Ernst, M.A. Sande, Correlation of *in vitro* time-kill curves and kinetics of bacterial killing in cerebrospinal fluid during ceftriaxone therapy of experimental *Escherichia coli* meningitis, Antimicrob. Agents Chemother. 24 (4) (1983) 463–467.
[27] L. Cai, J.J. Cai, H.P. Liu, D.Q. Fan, H. Peng, K.J. Wang, Recombinant medaka (*Oryzias melastigmus*) pro-hepcidin: multifunctional characterization, Comp. Biochem. Physiol. Part B Biochem. Mol. Biol. 161 (2012) 140–147.
[28] L. Li, J. Sun, S.F. Xia, X. Tian, M.J. Cheserek, G. Le, Mechanism of antifungal activity of antimicrobial peptide APP, a cell-penetrating peptide derivative, against *Candida albicans*: intracellular DNA binding and cell cycle arrest, Appl. Microbiol. Biotechnol. 100 (7) (2016) 3245–3253.
[29] L. Song, C. Lin, H. Gong, C. Wang, L. Liu, J. Wu, et al., miR-486 sustains NF-κB activity by disrupting multiple NF-κB-negative feedback loops, Cell Res. 23 (2) (2013) 274–289.
[30] K. Maruyama, T. Kawagoe, T. Kondo, S. Akira, O.T.R.A.F. Takeuchi, Family member-associated NF-κB activator (TANK) is a negative regulator of osteoclastogenesis and bone formation, J. Biol. Chem. 287 (34) (2012) 29114–29124.
[31] N. Mukaida, A. Harada, K. Matsushima, Interleukin-8 (IL-8) and monocyte chemotactic and activating factor (MCAF/MCP-1), chemokines essentially involved in inflammatory and immune reactions, Cytokine & Growth Factor Rev. 9 (1) (1998) 9–23.
[32] P.H. Schafer, A. Parton, L. Capone, D. Cedzik, H. Brady, J.F. Evans, et al., Apremilast is a selective PDE4 inhibitor with regulatory effects on innate immunity, Cell. Signal. 26 (9) (2014) 2016–2029.
[33] T.M. Watchorn, I. Waddell, N. Dowidar, J.A. Ross, Proteolysis-inducing factor regulates hepatic gene expression via the transcription factors NF-κB and STAT3, FASEB J. 15 (3) (2001) 562–564.
[34] J. Rothe, W. Lesslauer, H. Lötscher, Y. Lang, P. Koebel, F. Köntgen, et al., Mice lacking the tumour necrosis factor receptor 1 are resistant to IMF-mediated toxicity but highly susceptible to infection by Listeria monocytogenes, Nature 364 (6440) (1993) 798–802.
[35] A.T. Gewirtz, T.A. Navas, S. Lyons, P.J. Godowski, J.L. Madara, Cutting edge: bacterial flagellin activates basolaterally expressed TLR5 to induce epithelial proinflammatory gene expression, J. Immunol. 167 (4) (2001) 1882–1885.

[36] J.H. Cho, B.H. Sung, S.C. Kim, Buforins: histone H2A-derived antimicrobial peptides from toad stomach, Biochimica Biophys. Acta (BBA)-Biomembr. 1788 (8) (2009) 1564–1569.
[37] Y.S. Koo, J.M. Kim, I.Y. Park, B.J. Yu, S.A. Jang, K.S. Kim, et al., Structure-activity relations of parasin I, a histone H2A-derived antimicrobial peptide, Peptides 29 (7) (2008) 1102–1108.
[38] S. Thennarasu, R. Nagaraj, Specific antimicrobial and hemolytic activities of 18-residue peptides derived from the amino terminal region of the toxin pardaxin, Protein Eng. 19 (12) (1996) 1219–1224.
[39] K.H. Lee, S.Y. Hong, J.E. Oh, B.J. Lee, B.S. Choi, Antimicrobial activity and conformation of Gaegurin-6 amide and its analogs, Peptides 19 (10) (1998) 1653–1658.
[40] K. Pütsep, C.I. Brändén, H.G. Boman, S. Normark, Antibacterial peptide from *H. pylori*, Sci. Corresp. 398 (1999) 671–672.
[41] J.K. Lee, R. Gopal, S.C. Park, H.S. Ko, Y. Kim, K.S. Hahm, et al., A proline-hinge alters the characteristics of the amphipathic alpha-helical AMPs, PLoS One 8 (7) (2013) e67597.
[42] G. Hao, Y.H. Shi, Y.L. Tang, G.W. Le, The intracellular mechanism of action on *Escherichia coli* of BF2-A/C, two analogues of the antimicrobial peptide Buforin 2, J. Microbiol. 51 (2013) 200–206.
[43] J. Hong, W.T. Guan, G. Jin, H.Y. Zhao, X.H. Jiang, J.G. Dai, Mechanism of tachyplesin I injury to bacterial membranes and intracellular enzymes, determined by laser confocal scanning microscopy and flow cytometry, Microbiol Res. 170 (2015) 69–77.
[44] C.L. Friedrich, A. Rozek, A. Patrzykat, R.E.W. Hancock, Structure and mechanism of action of an indolicidin peptide derivative with improved activity against gram-positive bacteria, J. Biol. Chem. 276 (26) (2001) 24015–24022.
[45] M. Scocchi, M. Mardirossian, G. Runti, M. Benincasa, Non-membrane permeabilizing modes of action of antimicrobial peptides on bacteria, Curr. Top. Med. Chem. 16 (1) (2016) 76–88.
[46] Y.D. Wang, C.W. Kung, J.Y. Chen, Antiviral activity by fish antimicrobial peptides of epinecidin-1 and hepcidin 1-5 against nervous necrosis virus in medaka, Peptides 31 (6) (2010) 1026–1033.
[47] Y.C. Ding, X.M. Liu, L.Z. Bu, H.Y. Li, S.C. Zhang, Antimicrobial-immunomodulatory activities of zebrafish phosvitin-derived peptide Pt5, Peptides 37 (2) (2012) 309–313.
[48] Y.P. Lai, R.L. Gallo, AMPed up immunity: how antimicrobial peptides have multiple roles in immune defense, Trends Immunol. 30 (3) (2009) 131–141.